Human Myocardium: Single-Breath-hold MR T1 Mapping with High Spatial Resolution—Reproducibility Study[1]

Daniel R. Messroghli, MD
Sven Plein, MD
David M. Higgins, MSc
Kevin Walters, PhD
Timothy R. Jones, MSc
John P. Ridgway, PhD
Mohan U. Sivananthan, MD

A prospective study approved by the local ethics committee was performed to establish the normal range and reproducibility of myocardial T1 values as assessed with single-breath-hold T1 mapping with high spatial resolution. With a 1.5-T magnetic resonance (MR) imaging system, baseline and contrast material–enhanced modified Look-Locker inversion recovery, or MOLLI, imaging was performed in 15 healthy volunteers who had given written informed consent. Image quality scores and myocardial T1 values were derived for standard short-axis segments and sections. Results were compared with those from a second MR imaging study performed on the same day (baseline only) and those from a third study performed on a different day (baseline and contrast enhanced; eight volunteers). Intra- and interobserver agreement were determined. Myocardial T1 maps were obtained rapidly in a reproducible fashion. A normal range for baseline and postcontrast myocardial T1 was established (baseline mean T1 in short-axis sections, 980 msec ± 53 [standard deviation]; 95% confidence interval: 964, 997; number of sections, 43). This technique could enable direct quantification of changes in tissue characteristics in ischemic and inflammatory myocardial diseases.

[1] From the BHF Cardiac MRI Unit (D.R.M., S.P., T.R.J., M.U.S.) and Department of Medical Physics (D.M.H., J.P.R.), Leeds General Infirmary, Leeds, England; and Division of Genomic Medicine, University of Sheffield, Sheffield, England (K.W.). Received November 10, 2004; revision requested January 5, 2005; revision received February 15; accepted March 8; final version accepted May 2. D.M. supported by a Marie Curie Fellowship grant by the European Commission. **Address correspondence to** D.R.M., Cardiac MRI Unit, Franz-Volhard-Klinik, Charité, Campus Buch, Wiltbergstrasse 50, 13125 Berlin, Germany. (e-mail: *daniel.messroghli@charite.de*).

The longitudinal spin-lattice relaxation time (T1) is one of the principal tissue properties used for the generation of signal in magnetic resonance (MR) imaging. Because clinical MR imaging is based on the excitation of hydrogen protons, in vivo T1 of a given voxel is predominantly determined by its water and fat content. Although T1 values are not specific for particular tissues, each tissue exhibits values within a specific range (1).

Gadopentetate dimeglumine is a standard MR imaging contrast medium with predominantly extracellular distribution that acts by shortening T1 in its immediate proximity. The longitudinal relaxation rate (1/T1) is directly proportional to the tissue concentration of the contrast medium (2,3).

With T1-weighted imaging techniques, the analysis of wash-in and washout of gadopentetate dimeglumine has been shown to have high diagnostic value for both regional and global myocardial diseases. In patients with myocardial infarction, delayed enhancement identifies nonviable myocardium with high accuracy (4–6). In patients with acute viral myocarditis, with cardiac involvement from systemic sarcoidosis, or with inflammation caused by cardiotoxic chemotherapeutic agents, early global enhancement of the myocardium compared with the enhancement of skeletal muscle has been used as a marker of inflammatory activity (7–11).

Unlike computed tomography, with which Hounsfield units can be used as a reference scale for attenuation, with conventional (including T1-weighted) MR imaging techniques, signal intensity is expressed on an arbitrary scale that differs from one imaging examination to another and therefore is unsuitable for direct signal quantification. T1 mapping, in contrast, enables signal quantification (in milliseconds) on a standardized scale. In T1 mapping techniques, signal recovery after a preparation pulse is sampled during multiple measurements, and the associated relaxation time is calculated for every pixel of a parametric image referred to as a T1 map (12). For instance, if a T1 map instead of a conventional T1-weighted image were to be used, areas of delayed enhancement could be quantified not only in terms of their spatial extent but also in terms of the magnitude of their signal intensity (rather than in terms of a dichotomous differentiation between high and low signal intensity).

Until recently, techniques for T1 mapping of the myocardium were limited by poor spatial and/or temporal resolution, which restricted their clinical applicability (13,14). Modified Look-Locker inversion recovery (MOLLI), a pulse sequence scheme for cardiac MR imaging, now enables the performance of myocardial T1 mapping with high spatial resolution by using clinical 1.5-T MR imaging systems within a single breath hold (15). Before this technique can be used to assess T1 changes in patients with myocardial disease, the normal in vivo T1 behavior of human myocardium needs to be determined. Thus, the aim of this study was to prospectively evaluate the reproducibility of myocardial T1 at 1.5 T, as assessed with MOLLI, and to establish normal ranges for T1 in human myocardium at baseline and after the administration of contrast medium.

Table 1

Study Design

Type of Imaging and Short-Axis Level	Study 1	Study 2	Study 3
Baseline			
Basal	Not performed	Performed	Not performed
Midcavity	Performed	Performed	Performed
Apical	Not performed	Performed	Not performed
Contrast enhanced*			
Midcavity	Not performed	Performed	Performed

Note.—Study 1 and study 2 were performed on the same day; study 3 was performed a mean of 155 days ± 85 after studies 1 and 2.

* With acquisition of images 2, 4, 6, 8, 10, 15, and 20 minutes after a second injection of gadopentetate dimeglumine.

Materials and Methods

Volunteers

Fifteen healthy volunteers (nine men, six women; mean age, 33.1 years ± 8.5 [standard deviation]; age range, 21–49 years) were enrolled in the study, which was performed at the British Heart Foundation Cardiac MRI Unit in Leeds, England. The inclusion criteria were as follows: no history of cardiovascular or systemic disease, no history of infection within 3 weeks before MR imaging, resting blood pressure of 135/85 mm Hg or less, normal results at 12-lead electrocardiography (ECG), and no contraindication to MR imaging such as claustrophobia or presence of metallic implants. The study was approved by the local ethics committee, and written informed consent was obtained from all volunteers.

MR Imaging Protocol

All volunteers underwent two MR imaging examinations on the same day (study 1 and study 2). Eight randomly selected volunteers underwent another MR imaging examination (study 3) on a different day (see below). Body height, weight, and tympanic temperature were

Published online before print
10.1148/radiol.2382041903

Radiology 2006; 238:1004–1012

Abbreviations:
ECG = electrocardiography
MOLLI = modified Look-Locker inversion recovery

Author contributions:
Guarantors of integrity of entire study, D.R.M., M.U.S.; study concepts/study design or data acquisition or data analysis/interpretation, all authors; manuscript drafting or manuscript revision for important intellectual content, all authors; approval of final version of submitted manuscript, all authors; literature research, D.R.M., M.U.S.; clinical studies, D.R.M., S.P., T.R.J., M.U.S.; statistical analysis, D.R.M., D.M.H., K.W., M.U.S.; and manuscript editing, D.R.M., S.P., D.M.H., K.W., M.U.S.

Authors stated no financial relationship to disclose.

Table 2

Volunteer Characteristics

Volunteer No./ Sex/Age (y)	Height (cm)	Weight (kg)	Body Mass Index (kg/m^2)	Heart Rate (beats/min)			Body Temperature (°C)	
				Study 1	Study 2	Study 3	Studies 1 and 2*	Study 3
1/M/48	176	76	24.5	70	70	65	MD	36.6
2/F/23	169	73	25.6	75	75	ND	36.9	ND
3/F/45	156	49	20.1	70	75	ND	37.2	ND
4/M/26	190	64	17.7	70	65	ND	36.5	ND
5/F/27	157	50	20.3	70	70	60	36.7	36.2
6/M/33	190	94	26.0	80	80	ND	36.4	ND
7/M/32	187	85	24.3	55	55	60	36.4	37.0
8/M/34	176	86	27.8	65	60	ND	35.9	ND
9/M/33	178	103	32.5	70	75	ND	36.3	ND
10/F/35	165	63	23.1	80	75	ND	36.3	ND
11/F/26	170	58	20.1	90	90	95	37.6	37.7
12/M/49	178	85	26.8	65	65	70	36.0	37.1
13/M/35	179	79	24.7	50	50	45	36.8	36.8
14/M/30	184	95	28.1	60	60	65	36.9	36.9
15/F/21	175	62	20.2	75	75	90	37.1	36.3

Note.—Mean volunteer age was 33.1 years ± 8.5, while mean height was 175.3 cm ± 10.5, mean weight was 74.8 kg ± 16.7, and mean body mass index was 24.1 kg/m^2 ± 3.9. Mean heart rate was 69.7 beats per minute ± 10.1 at study 1, 69.3 beats per minute ± 10.3 at study 2, and 68.8 beats per minute ± 16.4 at study 3. Mean body temperature was 36.6°C ± 0.5 at studies 1 and 2 and 36.8°C ± 0.5 at study 3. ND = no data (study 3 was not performed in this volunteer).

* MD = missing data.

recorded before the start of studies 1 and 3.

All MR imaging examinations were performed with a 1.5-T MR imaging system (Gyroscan Intera CV; Philips, Best, the Netherlands) with Master gradients (30 mT/m, 150 [mT · m^{-1}]/msec). At the beginning of all studies, localizer images and breath-hold long-axis cine images (vector ECG-gated steady-state free precession; repetition time msec/echo time msec, 3.0/1.5; matrix, 144 × 150; section thickness, 7 mm; 30 phases) were acquired. Standard basal, midcavity, and apical short-axis section orientations were chosen by selecting the center three of five sections positioned in systolic long-axis views that covered the entire left ventricle from the mitral annulus to the tip of the apex (16).

T1 mapping.—The MOLLI pulse sequence was used as previously described (15). MOLLI is a single-section T1 mapping technique that consists of three inversion-recovery prepared ECG-synchronized Look-Locker experiments ("trains"), which are performed consecutively within one breath hold (in 16–20 seconds). Each of the three trains starts with an inversion pulse that uses a specific inversion time (100, 200, or 350 msec), after which multiple single-shot images are acquired in consecutive heartbeats. All images are acquired with the same trigger delay time in end diastole, with an acquisition time of 191 msec. The three trains (which yield three, three, and five images) result in a set of 11 source images, which are identical except for their different effective inversion times. By merging these source images (in inversion time order) into one data set, T1 values can be computed for every pixel with three-parameter curve fitting; a map of T1 in the imaging section can then be generated from these pixel values (17,18). Other pulse sequence parameters were as follows: balanced steady-state free precession readout; sensitivity encoding factor, 2.0; 3.9/1.95; field of view, 380 mm; matrix, 240 × 151; and section thickness, 8 mm.

A data pool that allowed comparison of baseline myocardial T1 values between all three short-axis levels was created so that we could assess agreement of baseline T1 values between repeated measurements (performed on the same day and on separate days) and compare agreement between postcontrast T1 measurements acquired on separate occasions. The protocols of the three studies involved T1 mapping of the midcavity short-axis view as their core element (Table 1), as detailed below.

Study 1.—Baseline MOLLI of the myocardium was performed in the midcavity short-axis view. The volunteer was then removed from the MR imaging unit.

Study 2.—Baseline MOLLI of the myocardium was performed for all three short-axis levels (midcavity, basal, and apical) within 1 hour after study 1. Then, gadopentetate dimeglumine (Magnevist; Schering, Berlin, Germany) was administered at a dose of 0.15 mmol per kilogram of body weight through a 20-gauge cannula placed in an antecubital vein. To enable our imaging protocol to be compatible with existing perfusion protocols, the dose of the contrast agent was given in two parts. After the first injection (0.05 mmol/kg; injection rate, 5 mL/sec; 10-mL saline flush) was administered, there was a 60-second pause (as required for first-pass perfusion imaging) before the second injection (0.1 mmol/kg) was administered. MOLLI was performed in the

midcavity short-axis view 2, 4, 6, 8, 10, 15, and 20 minutes after the second injection.

Study 3.—Baseline MOLLI of the myocardium was performed in the midcavity short-axis view a mean of 155 days ± 85 (range, 8–251 days) after the initial studies. Contrast agent was given in the same manner as described for study 2, and MOLLI was again performed in the same view at 2, 4, 6, 8, 10, 15, and 20 minutes.

Data Analysis

T1 maps from MOLLI image sets were automatically calculated off-line on a standard personal computer by using a customized T1 mapping software that was developed in house and written in IDL 6.0 (RSI UK, Berkshire, England); the T1 maps were stored in Digital Imaging and Communications in Medicine format. With this software and a 2.4-GHz processor, the computation of one T1 map took approximately 7 minutes.

For extraction of myocardial T1 values, endocardial and epicardial contours were manually traced on all T1 maps by an observer (D.R.M., with 5 years of experience in cardiac MR imaging), who used a commercial software package (Mass 5.0; Medis, Leiden, the Netherlands). Care was taken to exclude epicardial structures and blood pool from the contours. In all midcavity T1 maps from study 2, contours were also traced by a second observer (S.P., with 5 years of experience in cardiac MR imaging) and retraced by the first observer a mean of 59 days ± 3 after the first assessment. Both observers were blinded to the contours traced by D.R.M. the first time. The anterior point of insertion of the right ventricular free wall in the left ventricle was set as the reference point, and the myocardial circumference was divided into six (for basal and midcavity sections) or four (for apical sections) segments.

The image quality for all segments was visually rated by two observers (D.R.M. and S.P.) in consensus by using a scale in which a score of 3 indicated that image quality was good, with no artifacts; a score of 2, that image quality was satisfactory, with minor artifacts

Figure 1

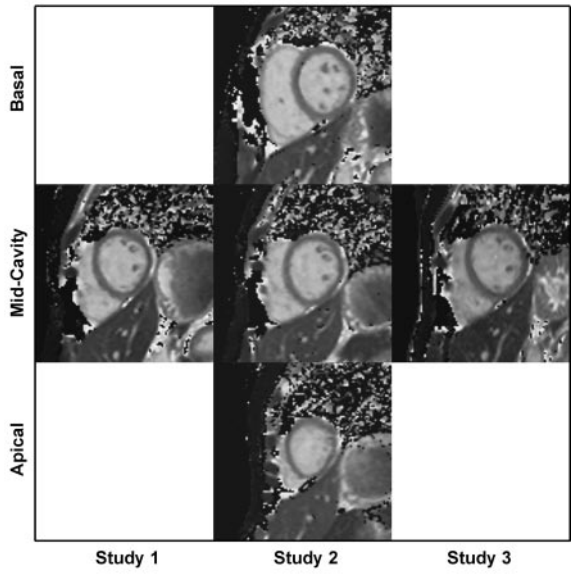

Figure 1: Representative baseline short-axis MOLLI T1 maps from all three studies in 27-year-old woman (volunteer 5). The spatial resolution (pixel size, 1.6 × 2.3 mm) is high enough to enable detection of left ventricular papillary muscles and trabeculations. Each of these maps was based on 11 steady-state free precession source MR images (3.90/1.95; flip angle, 50°; matrix, 240 × 151; section thickness, 8 mm).

Figure 2

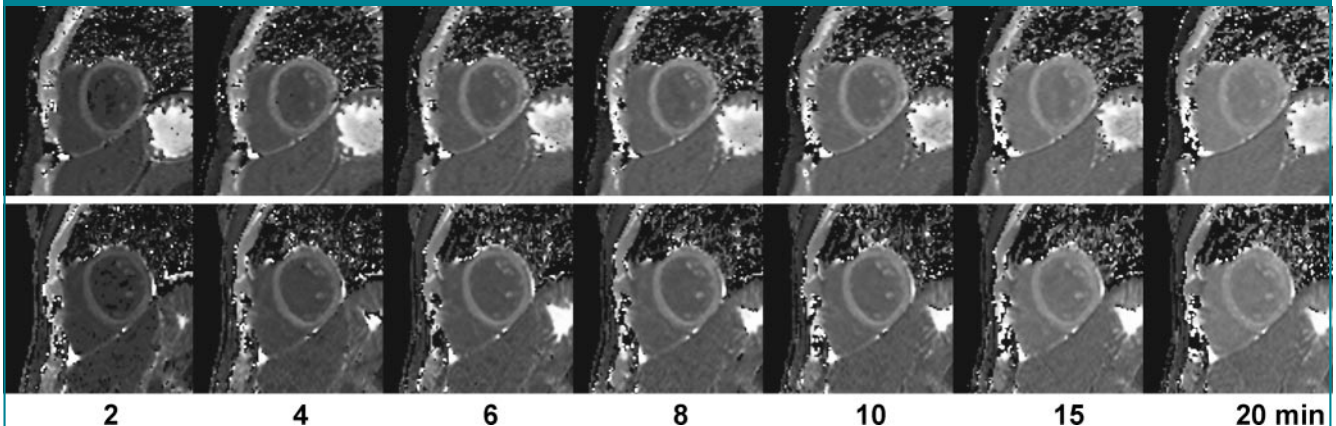

Figure 2: Representative postcontrast midcavity short-axis MOLLI T1 maps from study 2 (top) and 3 (bottom) in volunteer 5. Image quality is consistent for the full range of T1 values during washout of the contrast agent. Each of these maps was based on 11 steady-state free precession source MR images (3.90/1.95; flip angle, 50°; matrix, 240 × 151; section thickness, 8 mm).

(ie, artifacts that affected ≤ 3 adjacent pixels); and a score of 1, that an image was nonevaluable, with major artifacts (ie, artifacts that affected > 3 adjacent pixels). When artifacts were present, their cause (eg, insufficient breath holding, off-resonance effects) was determined through a review of the MOLLI source images. Segmental signal intensity reports were generated. The data were allocated to standard myocardial segments by using segments 1–16 of the 17-segment model recommended by the American Heart Association (19). T1 values from segments that were rated as nonevaluable were excluded from analysis. Image quality scores were derived for the basal, midcavity, and apical levels by averaging the segmental image quality ratings. Similarly, section T1 values were calculated by averaging the T1 values of the corresponding segments.

Table 3

Type and Frequency of Artifacts in Images of 1340 Cardiac Segments

Artifact Type	Appearance	Image Quality Grade*	
		2	3
Breathing	Diaphragm at different positions	3 (0.2)	28 (2.1)
Triggering	Left ventricle at different positions in different cardiac phases	0	6 (0.4)
Off resonance	Periodic signal distortions	4 (0.3)	5 (0.9)
Susceptibility	Focal signal loss, especially posterolateral close to great cardiac vein	12 (0.9)	5 (0.4)
Sensitivity encoding	Distortion along straight line crossing center of image	1 (0.1)	1 (0.1)
Ventricular motion	Blurry appearance of ventricular wall at high heart rates	18 (1.3)	12 (0.9)
Ghosting	Doubling of contours	2 (0.1)	1 (0.1)
Total		40 (3.0)	58 (4.3)

* Data are numbers of cardiac segments, with percentages in parentheses. An image quality grade of 2 indicated a satisfactory image with minor artifacts; and a grade of 3, a nonevaluable image with major artifacts. Image quality grades were assigned on the basis of artifact appearance in source images.

Statistical Analysis

Image quality scores for all volunteers were averaged for corresponding T1 maps. Frequency and types of artifacts were determined. Mean segmental and section T1 values ± standard deviations were calculated for all three studies.

For study 2, an analysis involving generalized estimating equations with a second-order stationary correlation structure was performed to compare baseline section T1 values derived from different short-axis levels within the volunteers and to account for possible section-level interdependencies.

For assessment of reproducibility, the agreement of measurements performed at different times and by different observers was determined by using the Pearson correlation and Bland-Altman analysis (20) for the following pairs of section T1 data sets: *(a)* baseline midcavity study 1 versus baseline midcavity study 2 (interstudy agreement, same day), *(b)* baseline and postcontrast midcavity study 2 versus baseline and postcontrast midcavity study 3 (interstudy agreement, different days), and *(c)* baseline midcavity study 2 results as assessed by a second observer and twice by the first observer (inter- and intraobserver agreement, respectively).

From results of in vitro studies in gel phantoms (15) it is known that T1 measurements—predominantly those for relatively long (>750 msec) and very short (<200 msec) T1 values—obtained with the MOLLI technique are subject to a mild systematic heart rate dependency. This is due to a variation in the timing of the readouts with respect to the inversion pulses at different heart rates because the imaging is ECG triggered. This variation introduces different degrees of disturbance of the longitudinal relaxation curve. The use of a balanced steady-state free precession readout sequence is a means to minimize these effects, which would be stronger if a conventional gradient-echo readout were used (21). Furthermore, the dose of the contrast agent is based on an individual's body weight, and variations in body habitus might therefore introduce differences in postcontrast T1. To find and correct for these potential confounding factors, the relationships between T1 and heart rate, height, and weight were investigated by using linear regression analysis of section data from study 2.

Coefficients of variation (COVs) were calculated with the following equation: $COV = (SD \cdot 100)/M$, where SD is the standard deviation and M is the mean value.

Generalized estimating equation analysis was performed by using Stata 8 (StataCorp, College Station, Tex); all other statistical analyses were performed by using Analyze-it 2002 (Analyze-it Software, Leeds, England). All tests were two tailed, and $P \leq .05$ was considered to indicate a significant difference.

Results

Volunteer characteristics are given in Table 2. One apical section (in volunteer 10) was inadvertently not acquired. As a result, 232 T1 maps that included 1362 segments were available for analysis.

Image Quality

Image quality was given a grade of 3 (good) for 1242 (92.7%) of the 1340 myocardial segments imaged in all three studies, a grade of 2 (satisfactory) for 40 (3.0%) segments, and a grade of 1 (nonevaluable) for 58 (4.3%) segments (Figs 1, 2). For study 2, the numbers of volunteers with at least one nonevaluable segment were five, four, and three for the basal, midcavity, and apical baseline sections, respectively. No volunteer had a nonevaluable segment in each section. The most frequently occurring artifacts (Table 3) were caused by respiratory or ventricular motion (32% and 31% of artifacts, respectively).

Myocardial T1 Values

Baseline segmental and section T1 values from study 2 are given in Figure 3 and Table 4, respectively. An analysis

performed by using generalized estimating equations revealed no significant difference between the mean T1 values derived for different baseline short-axis sections ($P = .423$). Figure 4 illustrates the recovery of absolute myocardial T1 in midcavity sections after the administration of the contrast agent.

Reproducibility

Evaluation of the reproducibility of T1 values assessed in the same section on the same day (for baseline studies), on a different day (for baseline and contrast-enhanced studies), and twice by the same observer or by a second observer (Table 5, Fig 5) revealed high agreement between baseline T1 values assessed twice on the same day or on different days and between postcontrast T1 values assessed on different days. Both intra- and interobserver agreement were high (mean difference, 2.6 msec ± 6.7 and −1.1 msec ± 8.9, respectively; Bland-Altman bias analysis).

Physiologic Covariates as Predictors of T1 Values

Univariate linear regression analyses were performed to determine if any of the physiologic covariates evaluated (heart rate, height, and weight) were significant explanatory variables at the 5% level. The only covariate that reached statistical significance was heart rate ($P < .001$) for baseline but not for contrast-enhanced T1 maps, indicating that $T1 = 790.4 + (2.7 \cdot HR)$, where HR is heart rate in beats per minute and 790.4 and 2.7 are constants that describe the relationship between corrected T1 ($T1_{corr}$) and raw (ie, uncorrected) T1 ($T1_{raw}$). Given this information, the equation $T1_{corr} = T1_{raw} - [2.7 \cdot (HR - 70)]$ was used to account for the dependence of baseline T1 on heart rate (70 beats per minute was the mean heart rate in our study). With this adjustment, baseline section T1 values were recalculated. Table 4 gives raw and heart rate–corrected values for baseline section T1. Although interstudy agreement on the same day (where the mean difference in heart rate was only 1.7 beats per minute) remained similar, agreement between studies performed on different days (where the mean difference in heart rate was 6.9 beats per minute) improved with heart rate correction (Table 5 and Fig 5).

The coefficient of variation was 5.4% for raw and 4.6% for heart rate–corrected pooled section T1 values.

Discussion

Our study involved a systematic analysis of the distribution and reproducibility of in vivo measurements of myocardial T1 obtained with a clinical MR imaging sys-

Figure 3

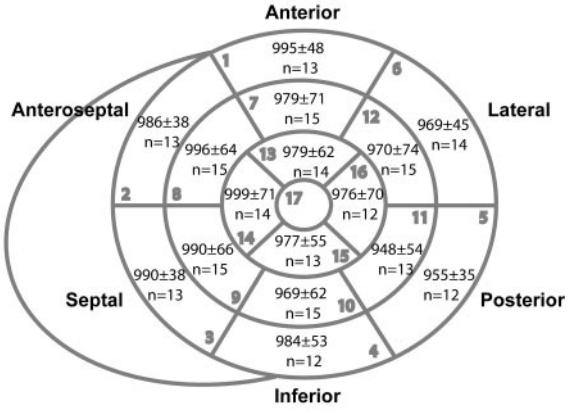

Figure 3: Distribution of baseline segmental raw T1 values (in milliseconds) in left ventricular myocardium in study 2. Values are expressed as means ± standard deviations. There was no significant difference in myocardial T1 values between basal, midcavity, and apical sections. Boldface numerals are segment numbers. *n* = number of segments available for evaluation.

Table 4

Baseline Section T1 Values before and after Heart Rate Correction

	Raw T1			Heart Rate–Corrected T1		
Short-Axis Level*	Mean ± SD	95% CI	Range	Mean ± SD	95% CI	Range
Basal ($n = 14$)	978 ± 36	957, 999	942–1081	978 ± 36	957, 999	929–1067
Midcavity ($n = 15$)	977 ± 63	942, 1011	887–1105	979 ± 54	949, 1008	915–1092
Apical ($n = 14$)	986 ± 60	951, 1021	862–1097	989 ± 47	962, 1016	902–1083
Total ($n = 43$)	980 ± 53	964, 997	862–1105	982 ± 46	968, 996	902–1092

Note.—Data are T1 values in milliseconds. CI = confidence interval, SD = standard deviation.

* Numbers are numbers of sections available for evaluation.

Figure 4

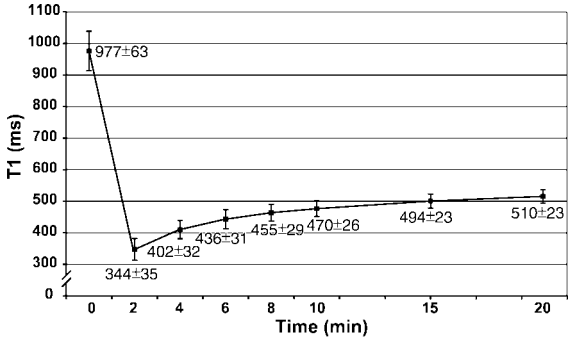

Figure 4: Graph shows recovery of absolute myocardial T1 in midcavity short-axis sections from study 2 from minute 0 (baseline raw value) to minute 20 after administration of 0.15 mmol/kg of gadopentetate dimeglumine. T1 values are expressed as means ± standard deviations. The exponential recovery of myocardial T1 reflects the washout of the contrast agent from the myocardium.

Table 5

Reproducibility of Midcavity Section T1 Values

Study[†]	Comparison: Study	Comparison: Time (min)[‡]	Correlation: Mean T1 ± SD (msec)[§]	Correlation: *r* Value	Bland-Altman Bias Analysis*: Difference ± SDD (msec)	Bland-Altman Bias Analysis*: Difference ± SDD[‖]	Bland-Altman Bias Analysis*: 95% CI (msec)
Same day							
(*n* = 15)	1 vs 2	0	962 ± 49	0.82	14.4 ± 34.7	1.5 ± 3.6	−5.2, 34.1
			977 ± 63				
		(0)	(963 ± 46)	(0.80)	(15.3 ± 32.0)	(1.6 ± 3.3)	(−2.8, 33.4)
			(979 ± 54)				
Different day							
(*n* = 8)	2 vs 3	0	959 ± 37	0.79	6.8 ± 28.1	0.7 ± 2.9	−16.6, 30.3
			966 ± 46				
		(0)	(967 ± 38)	(0.95)	(1.8 ± 12.6)	(0.2 ± 1.3)	(−8.8, 12.3)
			(969 ± 38)				
		2	347 ± 39	0.87	2.9 ± 21.0	0.8 ± 6.0	−14.6, 20.4
			350 ± 42				
		4	412 ± 29	0.84	−7.0 ± 18.0	1.7 ± 4.1	−22.1, 8.0
			405 ± 33				
		6	442 ± 26	0.82	−5.7 ± 14.6	−1.3 ± 3.3	−18.0, 6.6
			436 ± 21				
		8	461 ± 23	0.84	−7.9 ± 12.3	−1.7 ± 2.7	−18.2, 2.5
			453 ± 19				
		10	472 ± 25	0.79	−4.5 ± 15.4	−1.0 ± 3.3	−17.3, 8.4
			468 ± 18				
		15	493 ± 17	0.64	−3.1 ± 13.5	−0.6 ± 2.7	−14.4, 8.2
			490 ± 15				
		20	510 ± 19	0.39	0.1 ± 20.0	0.0 ± 3.9	−16.6, 16.8
			510 ± 17				
Intraobserver							
(*n* = 15)	2	0	977 ± 63	0.99	2.6 ± 6.7	0.3 ± 0.7	−1.2, 6.3
			979 ± 64				
Interobserver							
(*n* = 15)	2	0	977 ± 63	0.99	−1.1 ± 8.9	0.1 ± 0.9	−6.2, 3.9
			976 ± 65				

Note.—All results are derived from raw T1 values except for those in parentheses, which were derived from heart rate–corrected T1 values. CI = confidence interval, SD = standard deviation, SDD = standard deviation of difference. A study performed at 0 minutes was a baseline (nonenhanced) study.

* For results of Bland-Altman analysis, mean difference and standard deviation of the difference are given as actual values (in milliseconds) and as a percentage of the average of the two means.

[†] Values are numbers of volunteers.

[‡] A value of 0 indicates a baseline (nonenhanced) study.

[§] The first value given is that for the first of the two studies or sets of results being compared; the second is that for the second study or set of results. Heart rate–corrected values are given in similar fashion.

[‖] Given as a percentage of the average of the two means.

tem in healthy human myocardium. Our single-breath-hold T1 mapping approach yielded interpretable image quality for 95.7% of segments.

Baseline T1 values had narrow ranges and were similar at all three short-axis levels. Baseline and contrast-enhanced T1 measurements were reproducible when measured on separate occasions, as demonstrated by the relatively narrow confidence intervals calculated as part of Bland-Altman analysis. There was high intra- and interobserver agreement between the T1 measurements.

In addition to MOLLI, several other approaches have been adopted for assessing myocardial T1 at 1.5 T. Flacke et al (13) used a conventional inversion-recovery Look-Locker technique. Because image acquisition was performed continuously throughout the cardiac cycle, T1 could only be measured for regions of interest, which had to be traced manually on all source images. In a study by Wacker et al (14), T1 maps with a spatial resolution of 2.8 × 2.3 × 10 mm (compared with the resolution of 1.6 × 2.3 × 8 mm achievable with MOLLI) were generated by using a saturation-recovery technique. With a mean value of 980 msec ± 53, the raw baseline myocardial T1 observed in our study is in agreement with that in the study of Flacke et al (1033 msec ± 126) but lower than that in the study of

Wacker et al (1219 msec ± 72). The finding that our study yielded relatively low baseline T1 values is in agreement with results of previous phantom studies (15), which showed that with MOLLI there is a systematic underestimation of T1 by a magnitude of about 8%.

Of much greater importance for the differentiation between normal and pathologic states is the spread of the normal range of T1 values. Our study results indicate that, in terms of assessment of T1, MOLLI is comparable to the saturation-recovery technique, with a coefficient of variation for raw baseline T1 of 5.4% versus 5.9% (in five volunteers) in the study of Wacker et al (14). The variation with MOLLI is also comparable to or smaller than that reported for T1 measurements in different regions of the brain (22,23). Hence, there is no trade-off in terms of T1 precision for the high spatial resolution and high signal-to-noise ratio that distinguish MOLLI from other methods.

Although baseline T1 values were heart rate dependent, postcontrast T1 values were not. This finding is also in good agreement with findings in the phantom studies described above, which revealed that relevant heart rate effects with MOLLI are only to be expected for T1 values of less than 200 or more than 750 msec—values that are outside the range of postcontrast values for the myocardium seen in our study. Some degree of heart rate dependency is inevitable with MOLLI in its present form because such dependency is introduced by the single-shot readouts used. A simple heart rate correction of baseline T1 values could be performed in our study, and results of such correction were assessed along with the corresponding modified normal values. This correction for heart rate further reduced the spread of the normal range in our study population (coefficient of variation, 4.6%) and increased the reproducibility of measurements acquired on different days, on which differences in heart rate are common. Therefore, the use of heart rate correction for baseline myocardial T1 values should increase the sensitivity and specificity of this technique for future clinical applications. For automation, this correction could easily be integrated into the software that generates the T1 maps.

Figure 5

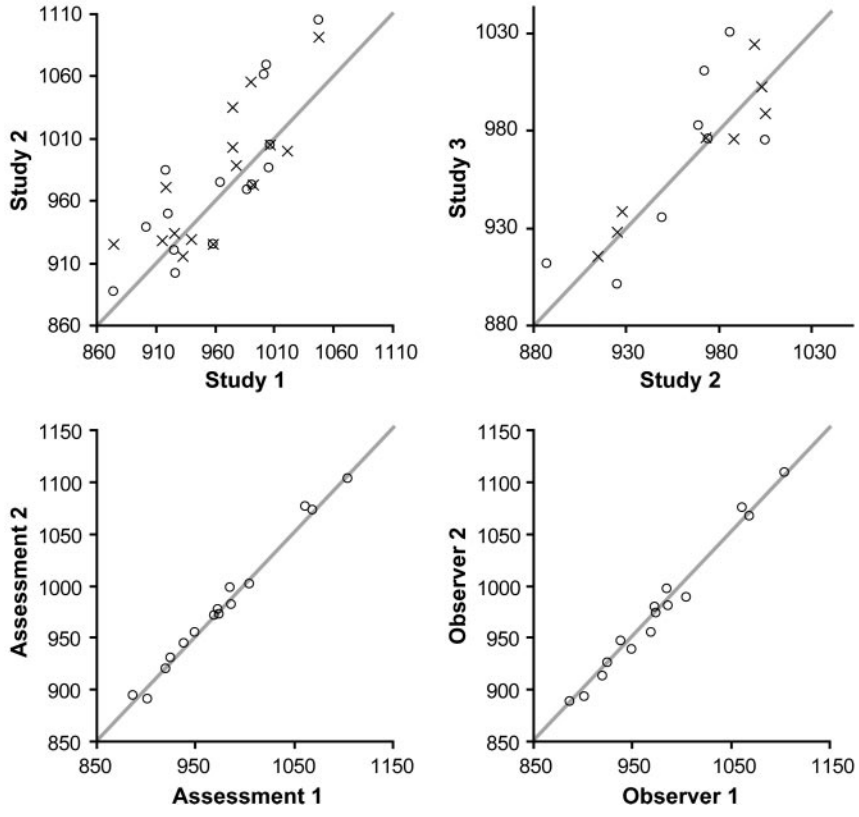

Figure 5: Scatterplots show same-day interstudy (upper left), different-day interstudy (upper right), intraobserver (lower left), and interobserver (lower right) agreement between baseline midcavity section myocardial T1 measurements (in milliseconds). Heart rate correction resulted in increased agreement between measurements obtained on different days. ○ = Raw T1, × = heart rate–corrected T1, line = line of identity.

Clinical Implications

Our results indicate that T1 mapping with high spatial resolution performed by using MOLLI is reproducible with a clinical MR imaging system. Therefore, fully quantitative analysis of myocardial T1 in a clinical setting becomes a realistic option. Focal changes in baseline T1 have been observed in patients with acute myocardial infarction (24). Signal quantification might further add to the diagnostic value of delayed enhancement imaging and would render adjustment of inversion times unnecessary. Global changes in the myocardium, such as those present in viral (7,11), immune-mediated (8,25), and drug-induced toxic (9) inflammation, may be able to be noninvasively demonstrated and quantified. This additional information may lead to the detection of myocardial involvement before functional parameters change. The diagnostic potential of MOLLI T1 mapping in these patient groups should be investigated in future studies.

Limitations

It is well known that T1 is dependent on temperature. A study in phantoms and animals at 1.5 T revealed that, between 32°C and 44°C, a 1% increase in T1 can be expected for each degree increase in body temperature (26). Because the range of body temperature in a healthy population is relatively small, it was not possible in our study to determine the exact influence of temperature on myo-

cardial T1 as assessed with MOLLI. For this purpose, larger studies with patients in hypo- and hyperthermic states would be necessary.

In our study, T1 was only derived for segments 1 through 16 of the left ventricle by using short-axis views. Segment 17 (the tip of the ventricular apex) can only be assessed with long-axis imaging. Assessment of right ventricular myocardium is technically challenging owing to the relative thinness of right ventricular walls and was not attempted in our study.

Breathing artifacts constituted a large proportion of the observed artifacts and frequently had detrimental effects on image quality for the affected myocardial segments. In these situations, the image quality of the T1 maps may have benefited if registration of the source images had been performed before the computation of pixel-by-pixel curve fittings. However, this would have required use of a dedicated software program, which was not available for our study; therefore, no such image registration was performed. Further reduction in motion artifacts might become possible in the future when shorter image acquisition times can be achieved by using advanced parallel imaging techniques with multichannel multicoil systems.

In conclusion, MOLLI T1 mapping enables quantification of myocardial T1 in a reproducible fashion. Heart rate correction further adds to the precision of baseline T1 measurements. The normal ranges for baseline and postcontrast T1 might serve as a basis for quantitative tissue characterization in clinical studies involving patients with myocardial infarction or inflammatory myocardial disease.

References

1. Bottomley PA, Foster TH, Argersinger RE, Pfeifer LM. A review of normal tissue hydrogen NMR relaxation times and relaxation mechanisms from 1–100 MHz: dependence on tissue type, NMR frequency, temperature, species, excision, and age. Med Phys 1984;11:425–448.
2. Nelson KL, Runge VM. Basic principles of MR contrast. Top Magn Reson Imaging 1995;7:124–136.
3. Weinmann HJ, Brasch RC, Press WR, Wesbey GE. Characteristics of gadolinium-DTPA complex: a potential NMR contrast agent. AJR Am J Roentgenol 1984;142:619–624.
4. Kim RJ, Chen EL, Lima JA, Judd RM. Myocardial Gd-DTPA kinetics determine MRI contrast enhancement and reflect the extent and severity of myocardial injury after acute reperfused infarction. Circulation 1996;94:3318–3326.
5. Judd RM, Lugo-Olivieri CH, Arai M, et al. Physiological basis of myocardial contrast enhancement in fast magnetic resonance images of 2-day-old reperfused canine infarcts. Circulation 1995;92:1902–1910.
6. Kim RJ, Wu E, Rafael A, et al. The use of contrast-enhanced magnetic resonance imaging to identify reversible myocardial dysfunction. N Engl J Med 2000;343:1445–1453.
7. Friedrich MG, Strohm O, Schulz-Menger J, Marciniak H, Luft FC, Dietz R. Contrast media-enhanced magnetic resonance imaging visualizes myocardial changes in the course of viral myocarditis. Circulation 1998;97:1802–1809.
8. Schulz-Menger J, Strohm O, Dietz R, Friedrich MG. Visualization of cardiac involvement in patients with systemic sarcoidosis applying contrast-enhanced magnetic resonance imaging. MAGMA 2000;11:82–83.
9. Wassmuth R, Lentzsch S, Erdbruegger U, et al. Subclinical cardiotoxic effects of anthracyclines as assessed by magnetic resonance imaging: a pilot study. Am Heart J 2001;141:1007–1013.
10. Wagner A, Schulz-Menger J, Dietz R, Friedrich MG. Long-term follow-up of patients with acute myocarditis by magnetic resonance imaging. MAGMA 2003;16:17–20.
11. Laissy JP, Messin B, Varenne O, et al. MRI of acute myocarditis: a comprehensive approach based on various imaging sequences. Chest 2002;122:1638–1648.
12. Kaldoudi E, Williams CR. Relaxation time measurements in NMR imaging. I. Longitudinal relaxation time. Concepts Magn Reson 1993;5:217–242.
13. Flacke SJ, Fischer SE, Lorenz CH. Measurement of the gadopentetate dimeglumine partition coefficient in human myocardium in vivo: normal distribution and elevation in acute and chronic infarction. Radiology 2001;218:703–710.
14. Wacker CM, Bock M, Hartlep AW, et al. Changes in myocardial oxygenation and perfusion under pharmacological stress with dipyridamole: assessment using T2* and T1 measurements. Magn Reson Med 1999;41:686–695.
15. Messroghli DR, Radjenovic A, Kozerke S, Higgins DM, Sivananthan MU, Ridgway JP. Modified Look-Locker inversion recovery (MOLLI) for high-resolution T1 mapping of the heart. Magn Reson Med 2004;52:141–146.
16. Messroghli DR, Bainbridge GJ, Alfakih K, et al. Assessment of regional left ventricular function: accuracy and reproducibility of positioning standard short-axis sections in cardiac MR imaging. Radiology 2005;235:229–236.
17. Nekolla S, Gneiting T, Syha J, Deichmann R, Haase A. T1 maps by K-space reduced snapshot-FLASH MRI. J Comput Assist Tomogr 1992;16:327–332.
18. Deichmann R, Haase A. Quantification of T1 values by SNAPSHOT-FLASH NMR imaging. J Magn Reson 1992;96:608–612.
19. Cerqueira MD, Weissman NJ, Dilsizian V, et al. Standardized myocardial segmentation and nomenclature for tomographic imaging of the heart: a statement for healthcare professionals from the Cardiac Imaging Committee of the Council on Clinical Cardiology of the American Heart Association. Circulation 2002;105:539–542.
20. Bland JM, Altman DG. Statistical methods for assessing agreement between two methods of clinical measurement. Lancet 1986;1:307–310.
21. Scheffler K, Hennig J. T(1) quantification with inversion recovery TrueFISP. Magn Reson Med 2001;45:720–723.
22. van Walderveen MA, van Schijndel RA, Pouwels PJ, Polman CH, Barkhof F. Multislice T1 relaxation time measurements in the brain using IR-EPI: reproducibility, normal values, and histogram analysis in patients with multiple sclerosis. J Magn Reson Imaging 2003;18:656–664.
23. Haselgrove J, Hunte M, Hurh P, Steen RG. Direct comparison of two methods to measure T1: in vitro and in vivo values by echo-planar imaging and by segmented k-space imaging. Magn Reson Imaging 2004;22:291–298.
24. Messroghli DR, Niendorf T, Schulz-Menger J, Dietz R, Friedrich MG. T1 mapping in patients with acute myocardial infarction. J Cardiovasc Magn Reson 2003;5:353–359.
25. Been M, Thomson BJ, Smith MA, et al. Myocardial involvement in systemic lupus erythematosus detected by magnetic resonance imaging. Eur Heart J 1988;9:1250–1256.
26. Peller M, Kurze V, Loeffler R, et al. Hyperthermia induces T1 relaxation and blood flow changes in tumors: a MRI thermometry study in vivo. Magn Reson Imaging 2003;21:545–551.